A new look at driven magnetic reconnection at the terrestrial subsolar magnetopause

John C. Dorelli, Michael Hesse, Maria M. Kuznetsova, and Lutz Rastaetter

Community Coordinated Modeling Center (CCMC), Electrodynamics Branch, Laboratory for Extraterrestrial Physics, NASA Goddard Space Flight Center, Greenbelt, Maryland, USA

Joachim Raeder

Space Science Center, University of New Hampshire, Durham, New Hampshire, USA

Received 3 March 2004; revised 27 May 2004; accepted 23 August 2004; published 18 December 2004.

[1] The physics of steady driven magnetic reconnection at Earth's subsolar magnetopause is addressed. Three-dimensional, global magnetohydrodynamics (MHD) simulations of the magnetopause are compared with analytical solutions of the resistive MHD equations [*Sonnerup and Priest*, 1975] corresponding to magnetic field annihilation driven by an incompressible stagnation point flow. The simulations demonstrate that under steady southward interplanetary magnetic field conditions and when the plasma resistivity is spatially uniform, subsolar magnetopause reconnection occurs in long, thin Sweet-Parker current sheets via a flux pileup mechanism [*Sonnerup and Priest*, 1975; *Priest and Forbes*, 1986] (rather than in Petschek slow shock configurations). Magnetic energy piles up upstream of the magnetopause current sheet to accommodate the sub-Alfvénic solar wind inflow. The scaling of the pileup with Lundquist number, S, is consistent (approximately $\propto S^{1/4}$) with that predicted by the analytical, incompressible stagnation point flow solutions (though there are small corrections due to plasma compressibility in the simulations). Since there is a finite energy in the magnetosheath available to drive the magnetic pileup (and associated rapid magnetic reconnection), we expect the pileup to saturate and the reconnection rate to drop as the upstream plasma pressure drops to accommodate the pileup. Thus we expect the reconnection to stall, the rate vanishing in the limit $S \rightarrow \infty$. We discuss the role of Hall electric fields in allowing the magnetic pileup to saturate before the reconnection begins to stall, permitting Alfvénic reconnection to occur in thin current sheets in the limit $S \rightarrow \infty$. *INDEX TERMS:* 7835 Space Plasma Physics: Magnetic reconnection; 7843 Space Plasma Physics: Numerical simulation studies; 7827 Space Plasma Physics: Kinetic and MHD theory; 2724 Magnetospheric Physics: Magnetopause, cusp, and boundary layers; 2728 Magnetospheric Physics: Magnetosheath; *KEYWORDS:* magnetic reconnection, magnetopause, magnetic flux pileup, global MHD simulation, GGCM

Citation: Dorelli, J. C., M. Hesse, M. M. Kuznetsova, L. Rastaetter, and J. Raeder (2004), A new look at driven magnetic reconnection at the terrestrial subsolar magnetopause, *J. Geophys. Res.*, *109*, A12216, doi:10.1029/2004JA010458.

1. Introduction

[2] Over the last 40 years, prodigious observational evidence has confirmed Dungey's [*Dungey*, 1961] reconnecting magnetosphere model. The existence of the polar rain and wind, the plasmapause, and the auroral oval all point directly to an open magnetosphere and thus indirectly to magnetic reconnection (see the review by *Kennel* [1995]). The ISEE spacecraft provided the first in situ evidence [*Paschmann et al.*, 1979] that something like Petschek's [*Petschek*, 1964] mechanism, i.e., plasma being accelerated to Alfvénic velocities by the "magnetic slingshot" produced by the component of the magnetic field (B_n) normal to the magnetopause surface, is operating at the dayside magnetopause. Since then, observations of the expected signatures of particle acceleration across rotational discontinuities have been interpreted as direct evidence for magnetic reconnection at the dayside magnetopause [*Cowley*, 1980; *Cowley*, 1982; *Gosling et al.*, 1990; *Sonnerup*, 1995; *Paschmann*, 1997; *Onsager and Lockwood*, 1997]. More recently, spacecraft instruments with higher spatial and temporal resolutions than those aboard the ISEE spacecraft have detected kinetic signatures (e.g., Hall electric fields and nongyrotropic electron velocity distributions) of collisionless reconnection at the magnetopause [*Mozer et al.*, 2002; *Scudder et al.*, 2002; *Mozer et al.*, 2003] and in the plasma sheet [*Oieroset et al.*, 2001].

[3] Unfortunately, owing to the computational challenges involved in accurately modeling processes occurring on disparate spatial and temporal scales in collisionless astrophysical plasmas, theoretical developments have been gen-

0148-0227/04/2004JA010458$09.00

erally confined to spatially localized regions with idealized geometries. For example, particle-in-cell (PIC) models of the magnetopause are generally confined to one and two spatial dimensions (see, for example, *Omidi and Winske* [1995] and *Lin* [2001]), and three-dimensional PIC simulations (see, for example, *Drake et al.* [2003]) are confined to spatial domains which cover only several ion inertial lengths. Resistive magnetohydrodynamics (MHD) is still the preferred approach to three-dimensional, global modeling of the magnetosphere; nevertheless, resistive MHD suffers from well-known deficiencies, particularly with respect to its ability to model magnetic reconnection in the low plasma resistivity limit. It is now clear (see, for example, *Biskamp* [1986] and *Biskamp and Schwarz* [2001]) that Petschek's reconnection mechanism is only relevant when the plasma resistivity is spatially localized in such a way that the spatial scale of the current layer is proportional to the magnitude of the resistivity (as assumed in Petschek's model). Without such spatial localization (e.g., if the plasma resistivity is spatially uniform), reconnection is typically observed to occur in long, thin Sweet-Parker current sheets [*Sweet*, 1958; *Parker*, 1957]. There are interesting questions surrounding the breakdown of the Petschek model in the constant resistivity case; for example, while Biskamp has argued that flux pileup reconnection is relevant whenever the driving inflow exceeds the Sweet-Parker velocity [*Biskamp*, 1986], *Strachan and Priest* [1994] have obtained new "hybrid solutions" (exhibiting properties of both flux pileup and slow mode compression reconnection solutions) which, they argue, explain the "Sweet-Parker" scaling observed in Biskamp's numerical experiments. (Note that in what follows, we will refer to a reconnection time which scales like the square root of the Lundquist number as a "Sweet-Parker" scaling; the reader should keep in mind, however, that the existence of a long, thin "Sweet-Parker" current sheet does not in itself imply that the reconnection time scales like $S^{1/2}$). Unfortunately, the Sweet-Parker reconnection time scales like the square root of the Lundquist number, S ($S = 4\pi V_A \lambda/(c^2\eta)$, where V_A is the Alfvén speed, λ is a length scale characterizing the system, c is the speed of light, and η is the plasma resistivity). This poses a significant problem for modelers attempting to explain the transfer of energy from the solar wind plasma to the magnetospheric plasma via magnetic reconnection, since both plasmas are essentially collisionless (i.e., $S \rightarrow \infty$).

[4] A more serious problem with the flux pileup mechanism is its prediction that the current sheet thickness scales like $S^{-1/2}$; thus resistive MHD itself breaks down as the sheet thickness approaches kinetic scales (e.g., particle Larmor radii), and a description in terms of the Vlasov equation is more appropriate. Again, owing to limited computational resources, electromagnetic PIC simulations of collisionless magnetic reconnection have largely focused on limited spatial and temporal domains (typically several ion inertial lengths in extent), using rather idealized equilibrium initial conditions to study various current driven plasma instabilities [*Horiuchi et al.*, 2001; *Hesse et al.*, 2001b; *Lapenta et al.*, 2003; *Li et al.*, 2003; *Daughton*, 2003]. Much larger three-dimensional "mesoscale" simulations, with system sizes of $\approx$100 d_i (where d_i is the ion inertial length), are possible using two-fluid codes [*Shay et al.*, 2003] but important kinetic effects which allow magnetic reconnection to occur, such as finite Larmor radius effects [*Hesse et al.*, 1999; *Kuznetsova et al.*, 2001] and anomalous resistivity associated with microturbulence [*Drake et al.*, 2003] are neglected in such calculations. While there is some evidence from simulations that ion inertial effects, in particular Hall electric fields, permit magnetic reconnection to occur at a rate which is insensitive to the electron dissipation mechanism [*Mandt et al.*, 1994; *Biskamp et al.*, 1995; *Ma and Bhattacharjee*, 1996; *Shay and Drake*, 1998; *Shay et al.*, 1999; *Hesse et al.*, 1999; *Kuznetsova et al.*, 2001; *Birn and Hesse*, 2001] the scaling of these results with "system size" (i.e, with d_i/λ) is controversial [*Wang et al.*, 2001; *Dorelli and Birn*, 2003; *Fitzpatrick*, 2003].

[5] In this paper we revisit the Sweet-Parker timescale problem in the context of steady, driven magnetic reconnection at the terrestrial subsolar magnetopause. We use global MHD simulations to demonstrate that if the plasma resistivity is spatially uniform, magnetic reconnection occurs in thin current sheets at a rate which is consistent with that predicted by analytical models of driven magnetic field annihilation (see, for example, *Sonnerup and Priest* [1975], *Watson and Craig* [1997], *Fabling and Craig* [1996], and *Craig et al.* [1997]). An important consequence of these scalings is that the reconnection rate approaches zero as the Lundquist number approaches infinity. Thus not unexpectedly, resistive MHD models with spatially uniform plasma resistivity are incapable of reproducing Dungey's reconnecting magnetosphere in the high Lundquist number limit. While recent theory [*Dorelli and Birn*, 2003; *Dorelli*, 2003] predicts that Hall electric fields can allow magnetic pileup to saturate before the reconnection stalls (i.e., before the reconnection rate begins to scale strongly with plasma resistivity), one expects a significant degree of pileup to occur under steady southward IMF conditions before the current sheet thickness approaches the ion inertial scale. This result is puzzling, given the fact that such magnetic pileup is rarely observed in the magnetosheath under southward IMF conditions [*Anderson et al.*, 1997]. We discuss several possible resolutions to this problem in the final section of this paper.

2. Driven Magnetic Field Annihilation

[6] In the context of solar-terrestrial physics, much of the research in reconnection physics is still motivated by the following, largely inaccurate view of two-dimensional reconnection theory: (1) the Sweet-Parker magnetic reconnection model cannot explain the "fast" (i.e., Alfvénic) timescales observed in such astrophysical dissipative events as solar flares and magnetospheric substorms; (2) the Petschek slow shock model solves the Sweet-Parker timescale problem, allowing magnetic energy dissipation to occur on Alfvénic timescales even as the Lundquist number, S ($S = 4\pi\lambda V_A/(\eta c^2)$, where λ is a system scale length, V_A is the Alfvén speed, η is the plasma resistivity, and c is the speed of light), approaches a realistic value (e.g., $S \approx 10^{13}$ in the solar corona). Parker himself [*Parker*, 1973] undermined 1 by showing how magnetic flux pileup can permit driven reconnection to occur at a rate which is independent of the Lundquist number. Biskamp's numerical experiments

[*Biskamp*, 1986; *Biskamp*, 1993] undermined 2 by showing that flux pileup reconnection (and not Petschek's slow shock configuration) seems to occur whenever the plasma resistivity is spatially uniform and the inflow exceeds the Sweet-Parker inflow speed (which scales like $S^{-1/2}$). In this work we present evidence that in the context of resistive MHD with constant plasma resistivity, magnetic reconnection at the terrestrial subsolar magnetopause occurs via the flux pileup mechanism, with magnetic energy being converted into plasma energy in thin current sheets of macroscopic length. Specifically, the bridge between the numerical experiments and the *Parker* [1973] solution is provided by *Sonnerup and Priest* [1975], who specialized Parker's solution to the case of unidirectional magnetic field line annihilation. Despite the simplification in magnetic field geometry, the Sonnerup and Priest solutions accommodated three dimensional flow fields, making them relevant to real astrophysical stagnation flows.

[7] While the Sonnerup and Priest annihilation solutions do not technically describe a reconnection process (since the current sheet is infinite and the magnetic field component normal to the sheet vanishes), we argue that the three-dimensional character of the stagnation point flow at the subsolar magnetopause makes the annihilation solutions more relevant to subsolar reconnection than the two-dimensional flux pileup reconnection solutions obtained by *Priest and Forbes* [1986]. For example, while the flux pileup solutions of *Priest and Forbes* [1986] are superior to the annihilation solutions, describing current sheets of finite length, they do not take into account the flow around the flanks of the magnetopause. This flow around the flanks of the magnetopause (which is included in the three-dimensional stagnation point flow solutions) significantly weakens the dependence of the magnetic flux pileup on the Lundquist number. Further, the magnitude of the magnetic field component normal to the current sheet is observed, in the simulations, to be much smaller than the magnitude of the reconnecting magnetic field just upstream of the sheet; thus away from the edges of the current sheet, the conversion of magnetic energy into plasma energy can be approximated as a driven annihilation process. As we demonstrate below, the Sonnerup and Priest solution makes a surprisingly accurate prediction of the scaling of the magnetic flux pileup with Lundquist number.

[8] Consider the steady state, incompressible MHD equations:

$$(\mathbf{U}\cdot\nabla)\boldsymbol{\omega} - (\boldsymbol{\omega}\cdot\nabla)\mathbf{U} = (\mathbf{B}\cdot\nabla)\mathbf{J} - (\mathbf{J}\cdot\nabla)\mathbf{B} \tag{1}$$

$$(\mathbf{U}\cdot\nabla)\mathbf{B} - (\mathbf{B}\cdot\nabla)\mathbf{U} = \frac{1}{S}\nabla^2\mathbf{B}, \tag{2}$$

where $\mathbf{U}$ is the bulk velocity, $\boldsymbol{\omega}$ is the vorticity ($\boldsymbol{\omega} = \nabla \times \mathbf{U}$), $\mathbf{B}$ is the magnetic field, $\mathbf{J}$ is the current density, and S is the Lundquist number. In the above equations (and in those which follow), all variables are dimensionless. Length scales are normalized by a characteristic system scale, λ; the magnetic field and the mass density are normalized by reference values, B_0 and ρ_0, respectively; the bulk velocity is normalized by the reference Alfvén speed, $V_A = B_0/\sqrt{4\pi\rho_0}$; the plasma pressure, p, is normalized by the magnetic energy density, $B_0^2/(8\pi)$; and the current density, $\mathbf{J}$, is normalized so that $\nabla \times \mathbf{B} = J$). Following *Sonnerup and Priest* [1975] and *Watson and Craig* [1997], we consider solutions with the form:

$$U_x = -U_0 x \tag{3}$$

$$U_y = U_0 y(1-\kappa) \tag{4}$$

$$U_z = U_0 z\kappa \tag{5}$$

$$B_x = 0 \tag{6}$$

$$B_y = 0 \tag{7}$$

$$B_z = f(x), \tag{8}$$

where U_0 is a constant which determines the strength of the driving flow, κ is a parameter controlling the anisotropy of the flow in the y–z plane (see Figures 4 and 5), and $f(x)$ gives the z component of the magnetic field as a function of x (i.e., normal to the one-dimensional current sheet).

[9] Figure 1 illustrates the three-dimensional stagnation flow annihilation solution of *Sonnerup and Priest* [1975]. The blue lines represent the magnetic field, which is being convected (the velocity field is represented by green arrows) toward a one-dimensional current sheet in the y–z plane at $x = 0$. The magnitude of the z component of the magnetic field, $f(x)$, satisfies the following equation:

$$\frac{1}{S}\frac{d^2 f}{dx^2} + U_0 x\frac{df}{dx} + U_0\kappa f = 0. \tag{9}$$

Anderson and Priest [1993] integrate equation (9) for the case $\kappa = 0$, noting that the general solution can be written in terms of the Kummer function, $M(a, b, x)$:

$$f(x) = c_0 Sx\exp\left(-SU_0\frac{x^2}{2}\right)M\left(\frac{1}{2},\frac{3}{2},SU_0\frac{x^2}{2}\right) + c_1\exp\left(-SU_0\frac{x^2}{2}\right), \tag{10}$$

where c_0 and c_1 are arbitrary constants. For arbitrary κ, *Craig et al.* [1997] note that the general solution of equation (9) can be written as follows:

$$f(x) = C_1 x(SU_0)^{1/2}M\left(\frac{\kappa+2}{2},\frac{3}{2},-SU_0\frac{x^2}{2}\right) + C_2 M\left(\frac{\kappa}{2},\frac{1}{2},-SU_0\frac{x^2}{2}\right). \tag{11}$$

For the case $C_2 = 0$ (i.e., the magnetic field vanishes at the stagnation point), one obtains pileup scaling laws from equation (11). If we fix the magnetic field magnitude, $|\mathbf{B}| = 1$, at $x = 1$, then $f(x)$ peaks at $x \equiv \ell \approx S^{1/2}$ and scales like $AS^{\kappa/2}x^{-\kappa}$ for large x. For example, Figure 2 shows the z component of the magnetic field, $f(x)$ for various values of S, with the flow anisotropy fixed. From equation (11), the local maximum of the magnetic field magnitude, $B_{\max} \equiv B_{\mathrm{up}}$, scales like $S^{\kappa/2}$. Thus if the outflow is parallel to the magnetic field (i.e., $\kappa = 1$), then $B_{\mathrm{up}} \propto S^{1/2}$. The pileup is most severe in this case, since the outflow does not transport magnetic flux away from the stagnation point. Further, the $S^{1/2}$ scaling of B_{up} compensates for the $U_{\mathrm{in}} \propto S^{-1/2}$ scaling

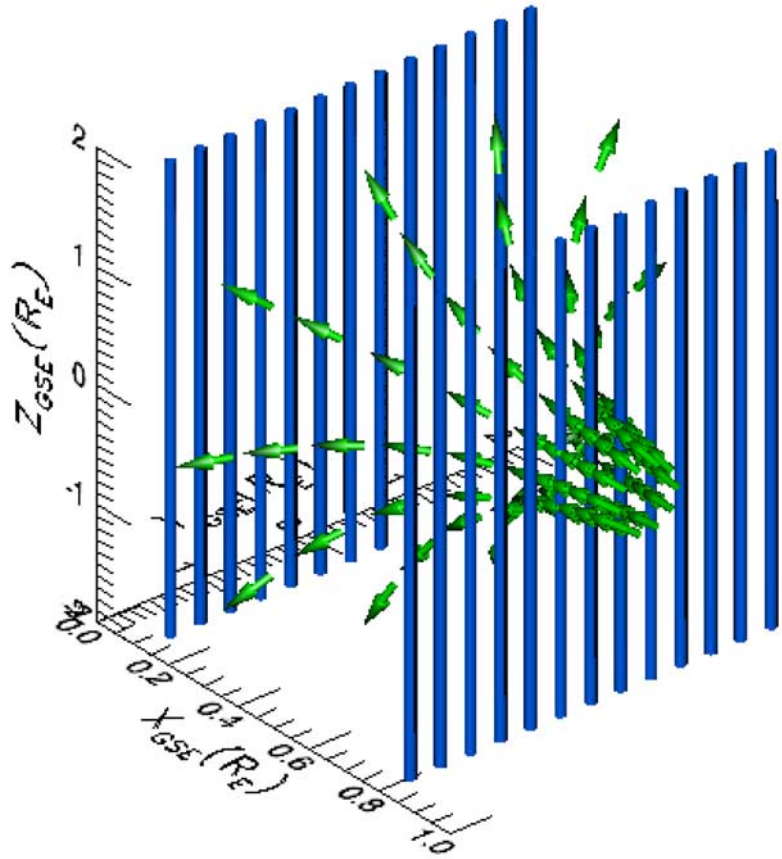

Figure 1. The three-dimensional annihilation solution of *Sonnerup and Priest* [1975]. Blue lines are magnetic field lines; green arrows show the bulk velocity vector field. The case shown here corresponds to $\kappa = 0.5$ (i.e., axisymmetric flow).

of the inflow (U_{in} is the magnitude of U_x at the location, ℓ, of the local maximum of B_z) so that the annihilation rate, $B_{up}U_{in}$, is independent of the Lundquist number.

[10] In contrast, when $\kappa = 0$ (i.e., the outflow is perpendicular to the magnetic field), there is no magnetic flux pileup for any value of S. In this case, the annihilation rate, $B_{up}U_{in}$, scales like $S^{-1/2}$. When the flow is axisymmetric ($\kappa = 1/2$), then $B_{up} \propto S^{1/4}$, and the annihilation rate scales like $S^{-1/4}$. Figure 3 shows the z component of the magnetic field for various values of κ, with the Lundquist number fixed.

[11] Figures 4 and 5 show the stagnation flow annihilation solutions for the two limiting cases: (1) $\kappa = 1$ (outflow parallel to the magnetic field) and (2) $\kappa = 0$ (outflow perpendicular to the magnetic field.) In the context of driven magnetic reconnection at the subsolar terrestrial magnetopause, the case $\kappa = 0$ would correspond to the situation where most of the magnetosheath inflow is diverted around the flanks of the magnetopause, while the case $\kappa = 1$ might be relevant in the situation where strong reconnection outflow diverts most of the magnetosheath inflow parallel to the magnetic field. In this work, we show that the actual situation in global MHD simulations, when the IMF is southward and thus favorable for magnetic reconnection at the subsolar point, is a combination of the two cases: (1) at the stagnation point, the flow is approximately axisymmetric (though there is a slight preference for the outflow to be around the flanks) and (2) at the northward and southward "edges" of the current sheet, where component of the magnetic field normal to the sheet is significant, the outflow is predominantly parallel to the magnetic field (as expected for an outflow driven by subsolar magnetic reconnection).

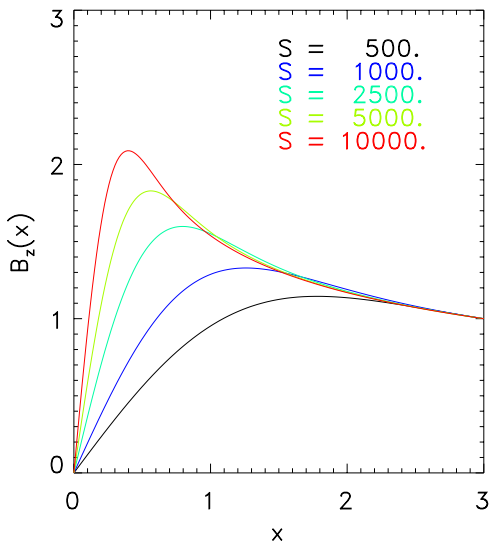

Figure 2. Magnetic energy pileup as a function of Lundquist number, S, for fixed flow anisotropy, $\kappa = 0.38$.

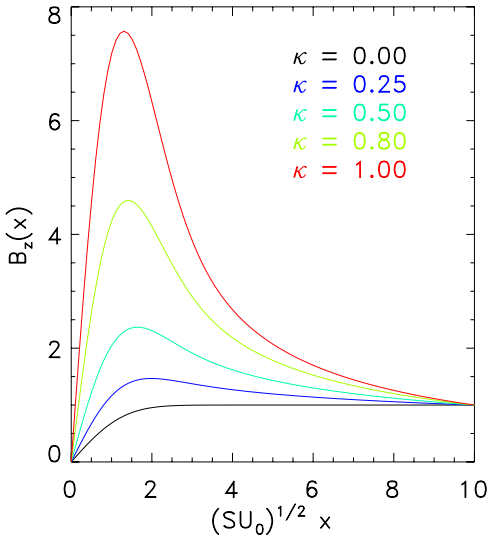

Figure 3. Magnetic energy pileup as a function of flow anisotropy, κ, for fixed Lundquist number, *S*.

Nevertheless, the degree of magnetic energy pileup along the Sun-Earth line is determined by the flow anisotropy upstream of the stagnation point not by the downstream reconnection-driven flow anisotropy.

[12] The κ = 1 stagnation point flow solution has been used to argue (see, for example, *Craig and Watson* [1999]) that Alfvénic reconnection is possible in thin current sheets even for astrophysically relevant Lundquist numbers (e.g., $S \approx 10^{13}$ in the solar corona). The essential idea is that although the speed at which magnetic flux is transported into the current sheet is inversely related to *S*, the magnetic flux just upstream of the current sheet is directly related to *S*. Thus magnetic flux pileup can compensate, to some extent, for the decrease in the inflow velocity with increasing *S*. For the case κ = 1, the pileup renders the reconnection rate independent of *S*, since $U_{in} \propto S^{-1/2}$ and $B_{up} \propto S^{1/2}$. For the axisymmetric case, κ = 1/2, $B_{up} \propto S^{1/4}$, implying that the annihilation rate decreases like $S^{-1/4}$ (which is significantly weaker than the Sweet-Parker scaling of $S^{-1/2}$).

[13] Unfortunately, as first recognized by *Priest* [1996], momentum conservation prevents the magnetic flux pileup from increasing indefinitely with increasing *S*. The three-dimensional stagnation point flow solutions of *Sonnerup and Priest* [1975] satisfy the following pressure balance condition (again, all variables are dimensionless):

$$p = \beta - B^2 - \rho U^2, \tag{12}$$

where β is the external plasma beta (the internal plasma energy density available to drive the magnetic field annihilation). Thus the external plasma beta sets an upper limit on the degree of magnetic energy pileup just upstream of the current sheet. *Litvinenko* [1999] computes an upper limit to the annihilation rate, E_y^{max}, based on the condition

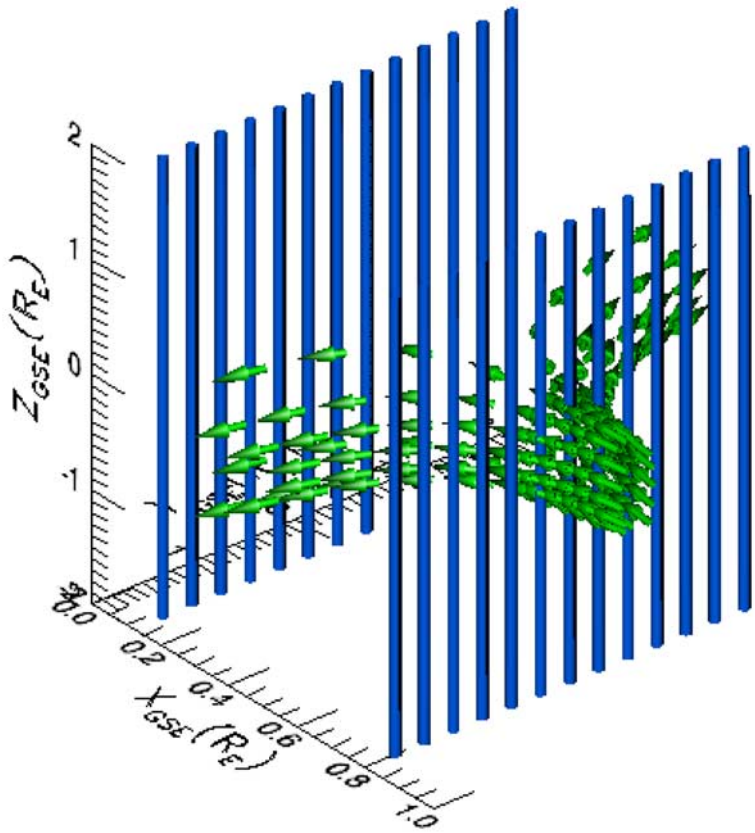

Figure 4. Three-dimensional annihilation solution for the case κ = 0.

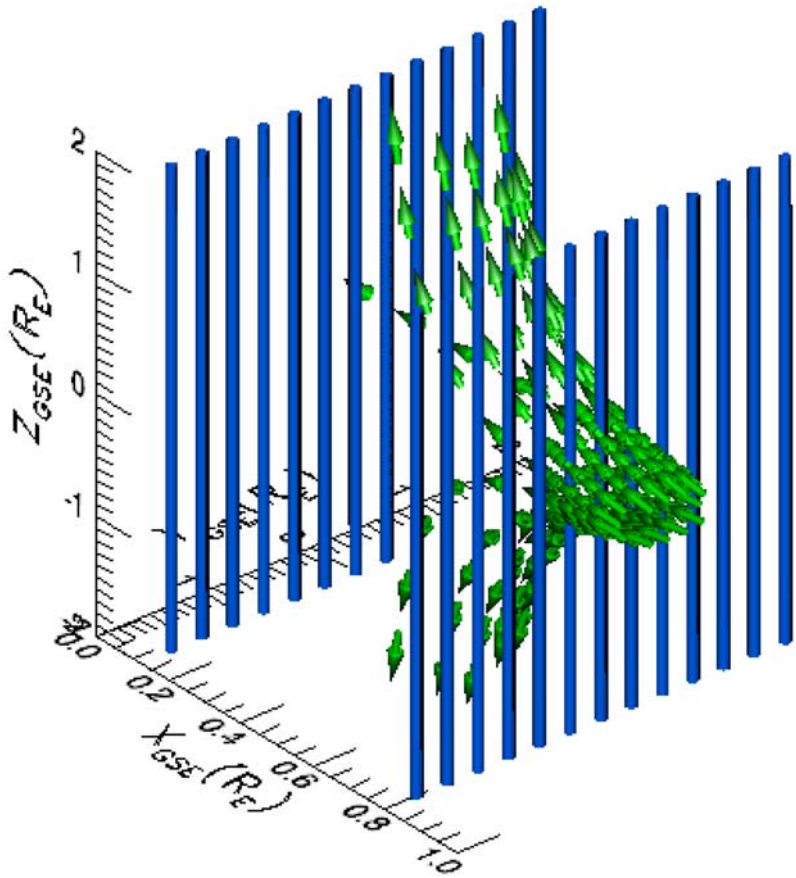

Figure 5. Three-dimensional annihilation solution for the case *kappa* = 1.

that the minimum pressure (consistent with the local maximum of the magnetic field) be positive. It turns out that $E_y^{\max} \propto S^{-1/2}$ so that the Sweet-Parker scaling reappears as an upper limit to the annihilation rate.

[14] In light of the discussion above, several questions arise when one addresses the problem of magnetic reconnection at the terrestrial subsolar magnetopause: When the plasma resistivity is constant in time and spatially uniform, does reconnection occur in macroscopic, thin current sheets, or is Petschek's slow shock mechanism relevant? If magnetic flux pileup reconnection is relevant, how do the magnetic energy pileup and reconnection electric field scale with plasma resistivity? What are the effects of Hall electric fields on the scaling of the reconnection rate with Lundquist number? We address the first two questions using global MHD simulations, demonstrating that flux pileup reconnection, and not Petschek's configuration, is relevant in the context of the terrestrial magnetopause when the plasma resistivity is spatially uniform. The third question is addressed using a Hall MHD generalization of the *Sonnerup and Priest* [1975] annihilation solution for the case $\kappa = 1$ (the case $\kappa \approx 1/2$ is more relevant for the three-dimensional (3-D) magnetopause, but it is not yet clear to us how to generalize that solution to include the effects of Hall electric fields. While *Sonnerup and Priest* [1975] point out that their solution can be extended to the case where the Hall term and the electron pressure gradient are included in Ohm's law, their solution does not model the quadrupolar "out-of-plane" magnetic field [*Mandt et al.*, 1994] which plays an important role in driving the reconnection process in whistler-mediated magnetic reconnection).

3. Global MHD Simulations

[15] The results presented in this paper were obtained using a version of the GGCM (Geospace General Circulation Model) code (developed by J. Raeder at University of California, Los Angeles) which is maintained at the Community Coordinated Modeling Center (CCMC) at the Goddard Space Flight Center. Details of the numerical methods are given elsewhere (see, for example, *Raeder* [1999]), but we will summarize the methods here. The code is parallelized, using the Message Passing Interface (MPI), to run on the Beowulf clusters at the CCMC.

[16] In the outer magnetosphere (outside a sphere of radius 3.5 R_E centered around Earth), the resistive MHD equations are solved using explicit finite difference schemes (to be described below):

$$\frac{\partial \rho}{\partial t} = -\nabla \cdot (\rho \mathbf{U}) \tag{13}$$

$$\frac{\partial \rho \mathbf{U}}{\partial t} = -\nabla \cdot -(\rho \mathbf{U}\mathbf{U} + p\mathbf{I}) + \mathbf{J} \times \mathbf{B} \tag{14}$$

$$\frac{\partial u}{\partial t} = -\nabla \cdot [(u + p)\mathbf{U}] + \mathbf{J} \cdot \mathbf{E} \tag{15}$$

$$\frac{\partial B}{\partial t} = -\nabla \times \mathbf{E} \tag{16}$$

$$\nabla \cdot \mathbf{B} = 0 \tag{17}$$

$$\mathbf{E} = -\mathbf{U} \times \mathbf{B} + \frac{1}{S}\mathbf{J} \tag{18}$$

$$\nabla \times \mathbf{B} = \mathbf{J} \tag{19}$$

$$u = \frac{1}{2}\rho U^2 + \frac{p}{\gamma - 1}, \tag{20}$$

where $\mathbf{I}$ is the unit tensor, u is the plasma energy density, $\mathbf{E}$ is the electric field, and γ is the ratio of specific heats (γ = 5/3 in this study). The variables are dimensionless, having been normalized as follows: spatial coordinates are normalized by 1 R_E; ρ is normalized by a reference value, $\rho_0 = 10^4$ cm^{-3}; the magnetic field, $\mathbf{B}$, is normalized by the magnitude of Earth's dipole field at 1 R_E; $\mathbf{U}$ is normalized by the reference Alfvén speed, $V_A = B_0/(4\pi\rho_0)^{1/2}$; u is normalized by the reference magnetic energy density, $B_0^2/(8\pi)$; t is normalized by the Alfvén time, $t_A = \lambda/V_A$ (where λ = 1 R_E); the current density, $\mathbf{J}$, and the electric field, $\mathbf{E}$, are normalized so that equations (18) and (19) are satisfied. The Lundquist number, S, is constant in time and spatially uniform (save for a spherical region of radius 6 R_E around Earth, where the resistivity is set to zero). The reader should note that S is defined here in terms of the reference magnetic field at 1 R_E, which is significantly higher than that in the magnetosheath. Thus we will distinguish between S and S_{MS} (the magnetosheath Lundquist number) when we discuss the magnetopause scaling results in the next section.

[17] Equations (13)–(20) are solved on a nonuniform rectangular mesh in GSE coordinates. In the y and z dimensions, the grid is exponential, extending out to ±48 R_E, with a minimum grid spacing of 0.15 R_E at $y = z = 0$. The magnetopause current sheet extends typically to a couple of Earth radii around the Sun-Earth line; the grid spacing at the "edges" of the current sheet is ≈0.3 R_E. In the x direction, the grid extends from 24 R_E on the dayside to −200 R_E in the tail; the grid is again nonuniform, with the resolution concentrated around the dayside magnetopause (several Earth radii around 8.5 R_E), where the resolution is ≈0.025 R_E. We have performed convergence tests to verify that the results we present in the following section are not sensitive to the grid resolution; nevertheless, we have determined that there is a measurable numerical resistivity in the highest Lundquist number run considered in this study (S = 10,000).

[18] As discussed by *Raeder* [1999], the gasdynamic part of the MHD equations, equations (13)–(15), are spatially discretized using a hybrid scheme in which fourth-order fluxes are combined with first-order Rusanov fluxes [*Harten and Zwas*, 1972] (with the Rusanov fluxes dominating in shock regions and the high-order fluxes dominating in smooth regions), while Faraday's law, equation (16), is discretized using the constrained transport method developed by *Evans and Hawley* [1988] (this method maintains $\nabla \cdot \mathbf{B} = 0$ to within round-off error). All of the equations are advanced in time using a second-order predictor-corrector scheme. The boundary conditions on the dayside are fixed in time, while those on the other five boundaries are free (i.e., normal derivatives vanish).

[19] Field-aligned currents (FAC), $J_\parallel$, are computed just outside a spherical region of radius 3.5 R_E, centered around Earth, and mapped to a spherical-polar ionospheric grid at 1 R_E using a dipole magnetic field model. The mapped FAC are used to compute the source term in the current continuity equation:

$$\nabla \cdot \boldsymbol{\Sigma} \cdot \nabla \Phi = -J_\parallel \sin I, \tag{21}$$

where Φ is the ionospheric potential on a spherical grid at 1 AU, $\boldsymbol{\Sigma}$ is a conductivity tensor, and I is the inclination of the dipole field at the ionosphere. Equation (21) is solved using a Galerkin pseudospectral method on a spherical-polar grid, with the boundary condition $\Phi = 0$ at the equator. The ionospheric conductivities include contributions from EUV ionization, diffuse auroral electron precipitation, and discrete aurorae associated with parallel electric fields (see *Raeder et al.* [2001] for details).

[20] In all of the runs described in this paper, the dipole tilt is set to zero and the following steady solar wind boundary conditions are imposed: the IMF is southward, with a magnitude of 5 nT; the solar wind speed is 400 km/s; the solar wind density is 5 cm^{-3}; the solar wind pressure is 7 pPa. We run the code long enough for a steady state to be reached on the dayside (typically this requires approximately 2 hours of simulated time). We present five runs, corresponding to the following set of Lundquist numbers: S = {500, 1000, 2000, 5000, 10,000}.

4. Results

[21] Figure 6 shows the magnetic field lines (red and blue lines) and bulk velocity field (green arrows) near the subsolar magnetopause for the case S = 10,000. The blue lines correspond to field lines for which the z component is negative ($B_z < 0$), and the red lines correspond to field lines for which $B_z > 0$. Comparing the figure with the axisymmetric stagnation flow solution (Figure 1), there are several immediately apparent differences: (1) The magnetic field lines are slightly draped around a curved magnetopause boundary; the solar wind appears to flow across a magnetic "hole" where the magnitude of the magnetic field is depressed (i.e., the flow does not appear to vanish at the magnetic null point); (2) The magnetic field has a component normal to the current sheet; the normal component is associated with magnetic reconnection, which is not present in the annihilation solution of Figure 1; (3) The outflow appears, at first glance, to be highly anisotropic, with the flow being predominantly parallel to the magnetic field downstream of the stagnation point (corresponding more closely to the κ = 1 case illustrated in Figure 5 than to the case illustrated in Figure 4); nevertheless, the bulk velocity field upstream of the stagnation point appears to be nearly axisymmetric.

[22] Figure 7 shows a slice of the current density in the noon-midnight meridional plane for the case S = 10,000. The Alfvén Mach number and plasma beta upstream of the current sheet (at ≈10 R_E) are ≈0.4 and 5, respectively. Qualitatively, the structure of the current layer, in particular,

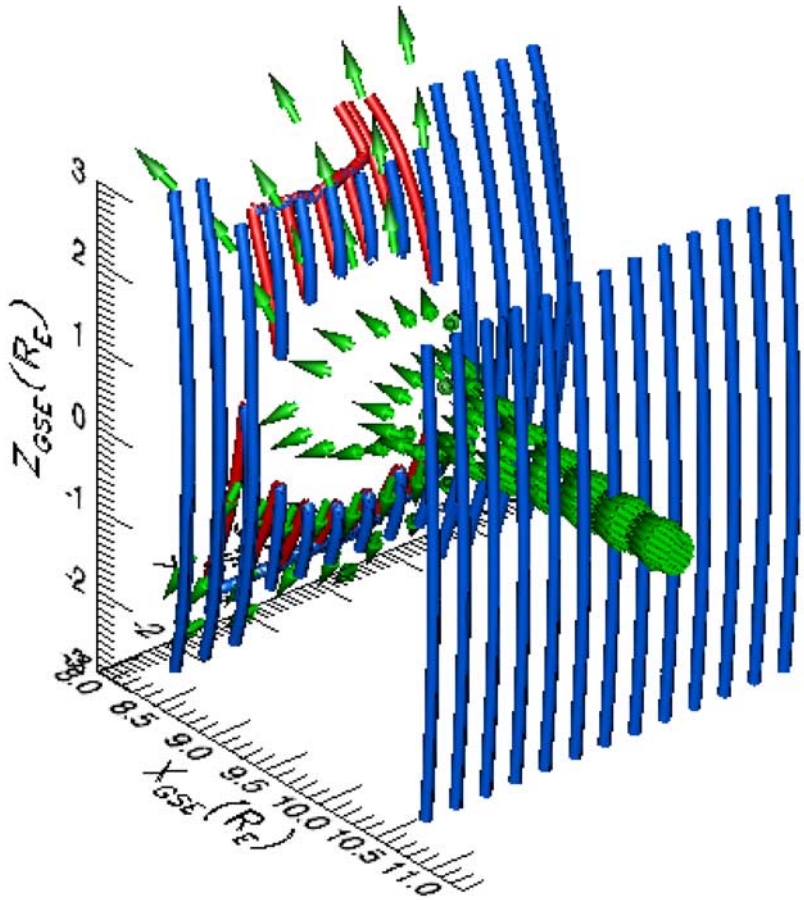

Figure 6. Three-dimensional view of the subsolar magnetopause for the case S = 10,000.

the large aspect ratio of the sheet, appears to be more consistent with the flux pileup theory [*Sonnerup and Priest*, 1975; *Priest and Forbes*, 1986] than with the Petschek theory. In particular, the length scale (in the z direction) of the sheet is macroscopic (being several Earth radii in length) while the thickness along the Sun-Earth line is about a tenth of an Earth radius. Further, we see no indication that the current sheet has disintegrated into a system of MHD discontinities (slow mode shocks, rotational discontinuities, and contact discontinuities), as predicted by Petschek-like theories where the dissipation is localized to a microscopic region around the stagnation point [*Heyn et al.*, 1988; *Heyn and Semenov*, 1996; *Semenov et al.*, 1998].

[23] Compare Figures 6 and 7, corresponding to the case S = 10,000, with Figures 8 and 9, corresponding to the case S = 5000. Again, magnetic dissipation appears to occur in a long, thin, Sweet-Parker like current sheet, with the outflow downstream of the stagnation point directed nearly parallel to the magnetic field. The aspect ratio of the current sheet is larger for the S = 10,000 case. Further, Figures 10 and 11 show that the magnetic flux pileup is more severe for the S = 10,000 case.

[24] It is interesting to note that the magnetic flux pileup in the S = 10,000 case is associated with a decrease in plasma pressure (about a 20% decrease) just upstream of the magnetopause current layer. This pressure decrease is a consequence of steady state pressure balance, as predicted by the *Sonnerup and Priest* [1975] annihilation solution. Figure 12 shows the plasma density in the noon-midnight meridion plane; it appears that the decrease in pressure upstream of the magnetopause is associated with a decrease in plasma density. While one might be tempted to identify this density decrease with the "plasma depletion layer" (PDL) often observed by spacecraft traversing the magnetopause under northward IMF conditions [*Crooker et al.*, 1979; *Song et al.*, 1992; *Anderson et al.*, 1997], and our results are indeed consistent with previous MHD simulations of the PDL [*Wu*, 1992; *Wang et al.*, 2003], *Song and Russell* [2002] point out that PDL layers observed by spacecraft typically involve larger decreases in plasma density (greater than 50%). We suggest that the density depletion observed in the simulations is a consequence of an adiabatic slow mode expansion associated with the pileup of magnetic flux upstream of the magnetopause current sheet (as argued by *Priest and Forbes* [1986]). In contrast, a Petschek reconnection configuration would be associated with a slow mode compression (and a corresponding decrease in the magnitude of the magnetic field just upstream of the magnetopause current layer). Thus the plasma depletion observed in the simulations is a consequence of pressure balance at the stagnation point in the presence of magnetic energy pileup. In other words, as the magnetic energy upstream of the current sheet increases, the plasma pressure decreases. We have confirmed that the plasma

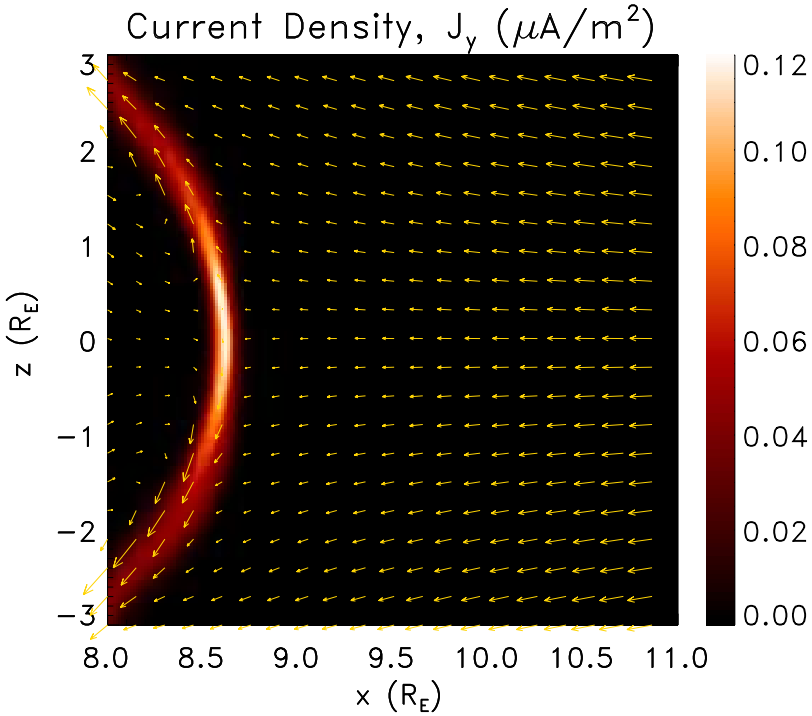

Figure 7. Current density in the noon-midnight meridional plane for the case S = 10,000. The bulk velocity field is shown with yellow arrows.

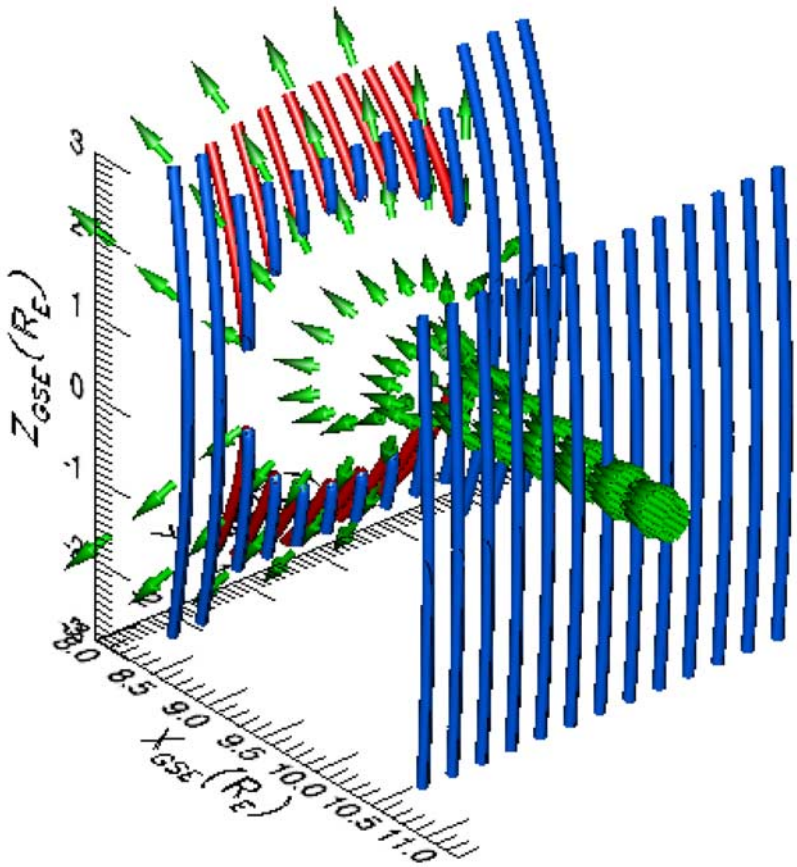

Figure 8. Three-dimensional view of the subsolar magnetopause for the case S = 5000.

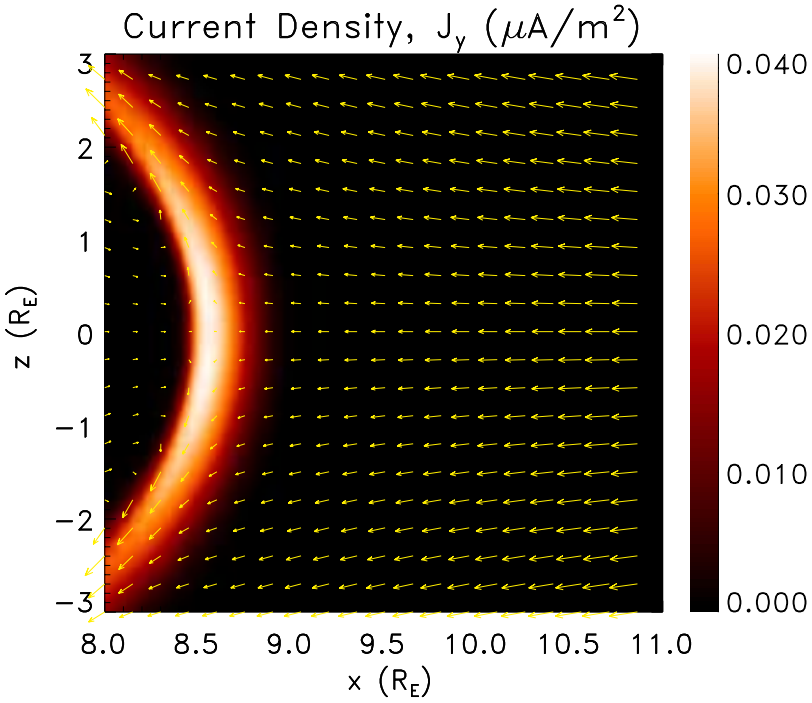

Figure 9. Current density in the noon-midnight meridional plane for the case $S = 5000$.

pressure in the magnetosheath (outside the current layer) is proportional to $\rho^{5/3}$. Since the plasma pressure must remain positive, the maximum possible amount of magnetic pileup must be bounded by the external plasma pressure available to drive the stagnation point flow. Thus as argued by *Priest* [1996] and *Litvinenko* [1999], the plasma pressure imposes a severe upper limit on the pileup reconnection rate which scales like $S^{-1/2}$. For the numerical experiments presented in this paper, the decrease in the upstream plasma pressure is small enough that we are not in the saturation regime.

[25] The three-dimensional stagnation point flow solution theory described in section 2 makes two simplifying assumptions which, it turns out, are not strictly valid in the global MHD simulations: (1) the plasma is incompressible and (2) the flow anisotropy, measured by the κ parameter in equations (4) and (5), is constant. Figure 13 shows the spatial variation of κ along the Sun-Earth line. The flow anisotropy, κ, was determined by computing the derivatives, $\partial U_y/\partial y$ and $\partial U_z/\partial z$, along the Sun-Earth line (it turns out that U_y and U_z are well approximated by linear functions of y and z, respectively, for some distance away from the Sun-Earth line). In the magnetosheath ($X \gtrsim 8.7\ R_E$), κ is approximately constant, in the range $0.4 \lesssim \kappa \lesssim 0.45$ (though for the $S = 10{,}000$ case, shown by the black curve, the flow anisotropy exhibits oscillatory behavior in the sheath; we have not yet investigated this interesting feature of the magnetosheath flow field geometry). As the flow crosses the current sheet ($X \approx 8.7\ R_E$), there is a rapid increase in the flow anisotropy. This increase in κ is a consequence of magnetic reconnection, which accelerates the plasma in the north-south direction at the edges of the current sheet. In previous numerical studies of flux pileup reconnection, *Dorelli and Birn* [2003] argued that away from the center of the current sheet, the magnetic pressure gradient along the sheet plays the dominant role in the acceleration process; along the center of the sheet, however, the plasma pressure gradient plays the dominant role. Thus plasma is squeezed out the ends of the sheet by the pressure gradient (magnetic and plasma) along the current sheet.

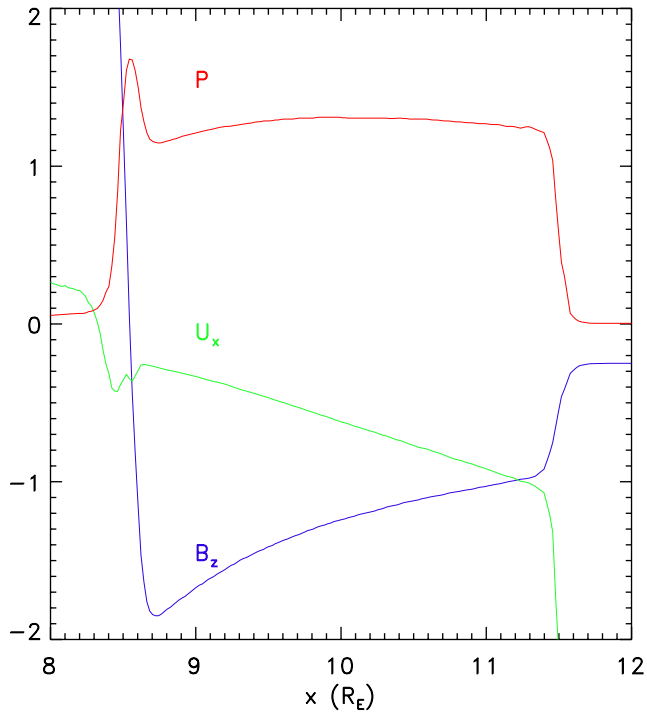

Figure 10. Magnetic flux pileup and associated plasma depletion along the Sun-Earth line for the case $S = 10{,}000$. The red line shows the plasma pressure; the green line shows the x component of the bulk velocity; the blue line shows the z component of the magnetic field.

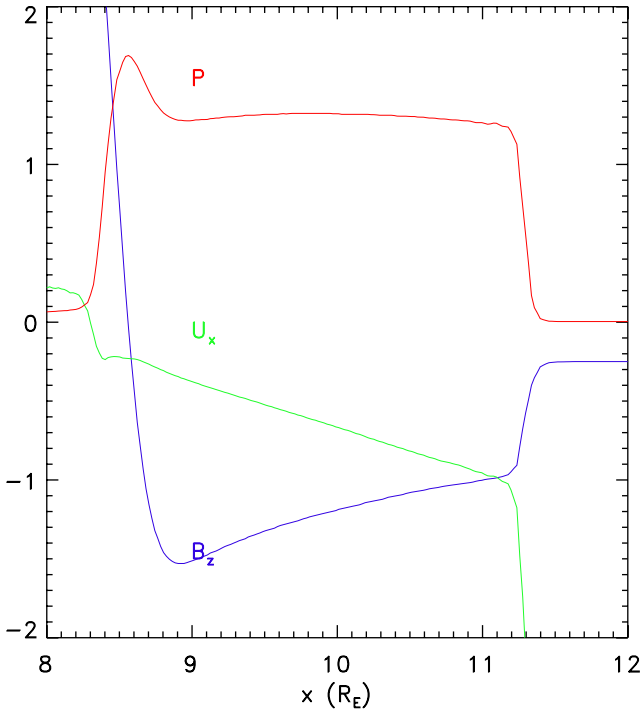

Figure 11. Magnetic flux pileup and associated plasma depletion along the Sun-Earth line for the case $S = 5000$.

Priest and Forbes [2000], on the other hand, point out that owing to the macroscopic length of the Sweet-Parker current sheet, the contribution to the $\mathbf{J} \times \mathbf{B}$ force of the component of the magnetic field normal to the current sheet cannot be neglected; thus one expects the outflow speed to be slightly greater than the upstream Alfvén speed, with both plasma pressure gradients and the magnetic tension force contributing to the plasma acceleration along the center of the sheet. A detailed analysis of the relative importance of the plasma pressure gradient and the $\mathbf{J} \times \mathbf{B}$ force along the simulated current sheets remains to be done.

[26] Interestingly, for the cases $S = 2000$ and $S = 5000$, there is a decrease in the flow anisotropy just upstream of the current sheet. The effect is most pronounced for the $S = 5000$ case and less obvious for $S = 2000$, and the effect is not observed in the $S = 10{,}000$ case. We are presently investigating the physical reasons for this decrease in the flow anisotropy; here, we tentatively suggest that as the plasma resistivity is decreased, reconnection in the thin current sheet is less efficient at accelerating magnetic flux downstream of the magnetic null or diffusing magnetic energy at the null. Thus more flux must be diverted around the flanks of the magnetopause, resulting in a decrease in the κ parameter. While this hypothesis seems intuitive, it does not explain why the increased flow around the flanks is not seen in the $S = 10{,}000$ case.

[27] Figure 14 compares the degree of magnetic pileup observed in the global MHD simulation with that expected from Faraday's law:

$$\mathbf{U} \cdot \nabla \mathbf{B} - \mathbf{B} \cdot \nabla \mathbf{U} + \mathbf{B}(\nabla \cdot U) - \frac{1}{S} \nabla^2 \mathbf{B} = 0. \qquad (22)$$

The solid lines in Figure 14 show the z component of the magnetic field, B_z, along the Sun-Earth line computed by the global MHD simulation. The dashed lines show B_z computed from the z component of equation (22) along the Sun-Earth line:

$$U_x \frac{\partial B_z}{\partial x} - C(x) B_z - \frac{1}{S} \frac{\partial^2 B_z}{\partial x^2} = 0 \qquad (23)$$

where $C(x) \equiv [\partial U_z/\partial z - \nabla \cdot \mathbf{U}]_{y=0,z=0}$. $U_x(x)|_{y=0,z=0}$ and $C(x)$ $C(x)$ are obtained from the simulations. Since $U(x)$ decreases linearly (to a good approximation) from the magnetosheath to the stagnation point along the Sun-Earth line and since the flow anisotropy is nearly constant in the sheath (see Figure 13), one might expect the degree of magnetic pileup observed in the simulations to agree quite well with that predicted by the theory of *Sonnerup and Priest* [1975]. Nevertheless, we have found that it is necessary to take into account plasma compressibility (the second term on the right-hand side of the definition of $C(x)$) in order to achieve the level of agreement demonstrated in Figure 14. The compressibility effect is negligible for the three lowest Lundquist number runs ($S = 500$, 1000, 2000), but it appears to be significant for the $S = 5000$ and $S = 10{,}000$ cases. For the $S = 10{,}000$ case, however, equation (23) systematically overestimates the degree of pileup when compared with the simulation results (compare the solid and dashed black lines in Figure 14). We have confirmed that this systematic error is caused by numerical diffusion, which implies that the "effective" Lundquist number for the $S = 10{,}000$ case is only slightly greater than 5000 (and spatially localized around the current sheet). This level of numerical resistivity is consistent with that observed in a previous study [*Raeder*, 1999].

[28] The effects of plasma compressibility and numerical resistivity on the *Sonnerup and Priest* [1975] solution can be seen clearly in Figure 15. The solid red line gives the prediction of the incompressible, constant κ theory of *Sonnerup and Priest* [1975] (where *kappa* = 0.4). The green

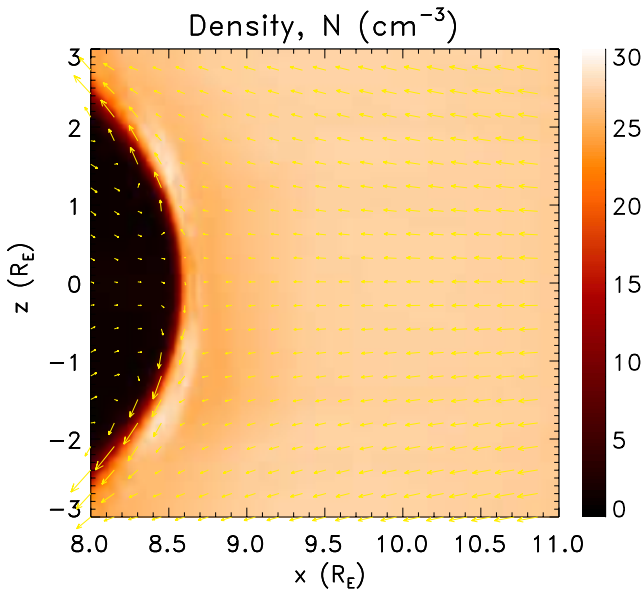

Figure 12. Density depletion upstream of the magnetopause for the case $S = 10{,}000$.

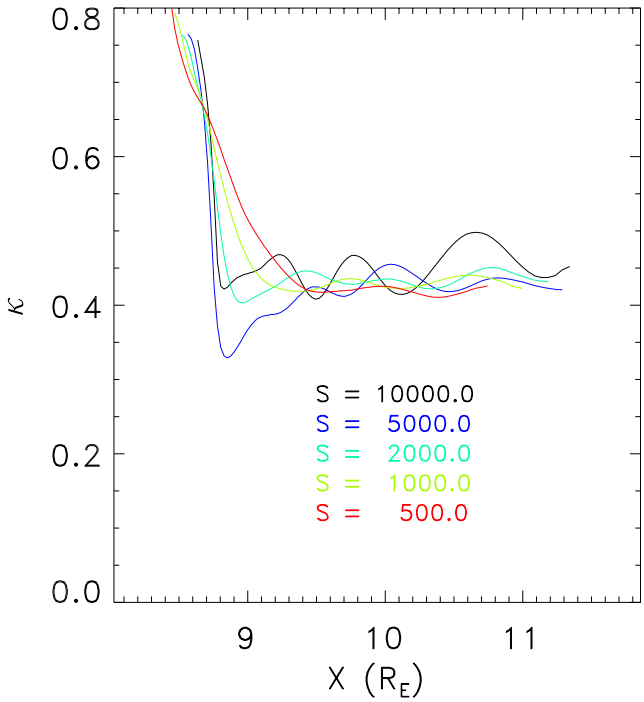

Figure 13. We plot the magnetosheath flow anisotropy, *kappa*, along the Sun-Earth line, for several values of the Lundquist number.

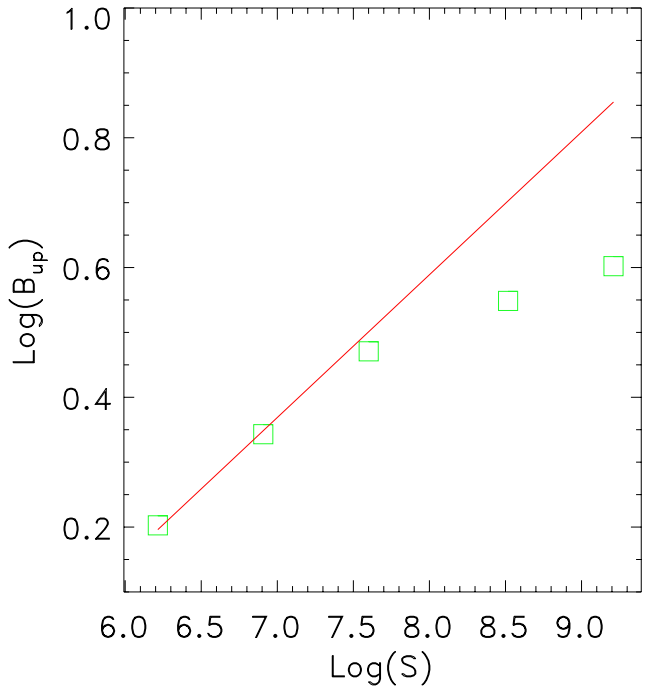

Figure 15. Scaling of magnetic flux pileup with Lundquist number. The red line shows the prediction of *Sonnerup and Priest* [1975] for the case $\kappa = 0.4$; the green squares show the simulation results.

squares show the simulation results. Consistent with Figure 14, the *Sonnerup and Priest* [1975] scaling ($B_{up} \propto S^{0.2}$) is obeyed for the lowest three Lundquist number cases. For the $S = 5000$ case, plasma compressibility results in less magnetic pileup than would be expected in the absence of incompressibility (numerical resistivity is insignificant for this case, as shown in Figure 14). It is difficult to separate the effect of plasma compressibility from numerical resistivity for the $S = 10{,}000$ case. Exactly why the plasma compressibility becomes more important at high Lundquist numbers, and why it has the effect of reducing the amount of magnetic pileup compared with that which would be expected in an incompressible plasma, is an interesting question which we must leave for the future.

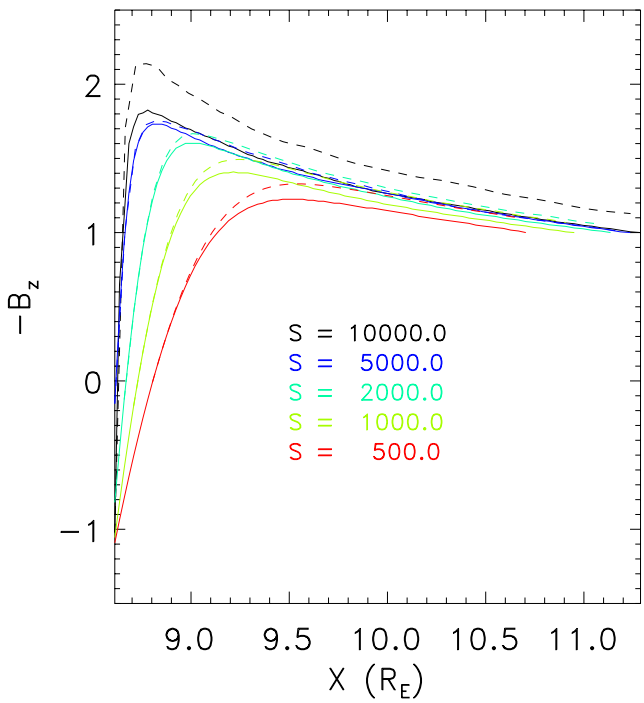

Figure 14. Here we compare B_z along the Sun-Earth line computed in the simulations (solid lines) with that predicted by equation (23) (dashed lines).

[29] Figure 16 shows the y component of the electric field at local maximum of the magnetic field, $E_y = -U_{in}B_{up}$, as a function of the Lundquist number. The solid red line shows the prediction of the incompressible *Sonnerup and Priest* [1975] theory with $\kappa = 0.4$ (i.e., the slope of the red line is $\kappa/2 = 0.2$). The green squares show the results of the global MHD simulations. Although the scaling observed in the simulation appears to be consistent with that predicted by the *Sonnerup and Priest* [1975] theory, one would expect to observe a change in scaling for the highest two Lundquist number cases ($S = 5000$ and $S = 10{,}000$) due to compressibility and numerical resistivity effects (as discussed above and illustrated clearly in Figure 15). Nevertheless, it seems as though the slight reduction in the level of magnetic pileup caused by plasma compressibility and numerical diffusion is compensated to some extent by a slightly larger than expected upstream bulk velocity. Further studies will be required in order to understand this effect.

5. Conclusions and Discussion

[30] We have revisited the reconnection timescale problem in the context of resistive magnetohydrodynamics (MHD) simulations of the terrestrial subsolar magneto-

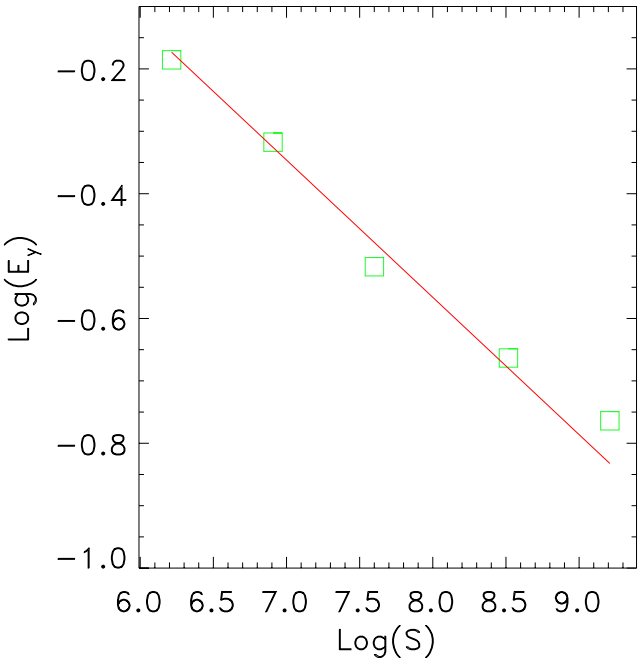

Figure 16. Dependence of reconnection electric field on Lundquist number. The red line shows the prediction of *Sonnerup and Priest* [1975] for the case $\kappa = 0.4$; the green squares show the simulation results.

pause. In particular, we have addressed the question of the scaling of magnetic reconnection with Lundquist number by computing a sequence of numerical solutions, using steady solar wind conditions with a southward interplanetary magnetic field configuration, for the following set of Lundquist numbers: $S = \{500, 1000, 2000, 5000, 10{,}000\}$. Our conclusions are summarized as follows.

[31] 1. When the plasma resistivity is constant (i.e., not current-dependent or spatially localized), driven subsolar reconnection occurs in thin current sheets of macroscopic length, rather than in Petschek-like configurations where slow shocks play a dominant role in the magnetic dissipation and plasma acceleration processes.

[32] 2. Magnetic energy piles up outside the current sheet to accommodate the magnetosheath flow; this magnetic pileup appears to be a ubiquitous feature of driven magnetic reconnection, having been observed in many previous driven reconnection scenarios [*Parker*, 1973; *Sonnerup and Priest*, 1975; *Biskamp*, 1986; *Wang et al.*, 1996; *Craig et al.*, 1997; *Watson and Craig*, 1997; *Dorelli and Birn*, 2003; *Dorelli*, 2003].

[33] 3. The scaling of magnetic pileup with Lundquist number observed in the MHD simulations is consistent with that predicted by the three-dimensional analytical stagnation point flow solutions of the resistive MHD equations [*Sonnerup and Priest*, 1975; *Craig et al.*, 1997; *Watson and Craig*, 1997].

[34] 4. The reconnection electric field, E_y, upstream of the current sheet is found to scale like $S^{-0.2}$, consistent with the prediction of the Sonnerup and Priest solution ($E_y \propto S^{-\kappa/2}$) with $\kappa = 0.4$ (which is the approximate value of κ observed in the simulations).

[35] 5. Plasma compressibility appears to reduce the amount of pileup required to support a given inflow, though it does not have as strong an impact on the scaling of E_y as it does on the scaling of B_{up}.

[36] 6. While the anisotropy of the inflow along the Sun-Earth line (as measured by the κ parameter in equations (4) and (5)) is only slightly less than 1/2 (i.e., the flow is nearly axisymmetric), the plasma pressure gradient and $\mathbf{J} \times \mathbf{B}$ forces along the current sheet accelerate the plasma out the ends of the sheet so that the flow is nearly parallel to the magnetic field downstream of the stagnation point.

[37] Conclusions 1–4 together provide strong evidence that in the context of resistive MHD, magnetic flux pileup reconnection in thin Sweet-Parker current sheets (rather than the Petschek slow shock model) is the relevant model of reconnection at the subsolar magnetopause when the plasma resistivity is constant. Thus since the magnetosheath flow is observed in the simulations to be nearly axisymmetric, we expect the reconnection rate to vanish in the limit $S \rightarrow \infty$. That is, without anomalous resistivity, which can enhance the reconnection rate either by decreasing S or spatially localizing it, global MHD simulations will likely not reproduce Dungey's open magnetosphere for large values of S.

[38] There are a number of possible approaches to solving the reconnection timescale problem implied by conclusions 1–4 above. One can categorize them as follows: (1) approaches which seek solutions of the resistive MHD equations such that the reconnection rate is insensitive to the Lundquist number, and (2) approaches which generalize Ohm's law to take into account kinetic scale physics which is neglected in the MHD approach. Both Petschek's model and the flux pileup models of *Sonnerup and Priest* [1975] and *Priest and Forbes* [1986] are examples of approaches in category 1. Petschek's model is problematic since it appears to be valid only when the plasma resistivity is spatially localized. Setting $\kappa = 0$ in the *Sonnerup and Priest* [1975] flux pileup model is not a viable solution, since there is a finite external pressure available to drive the magnetosheath stagnation point flow. Thus one expects the flux pileup to saturate at some critical value of the Lundquist number, above which the Sweet-Parker scaling reappears [*Priest*, 1996; *Litvinenko et al.*, 1996; *Litvinenko*, 1999]. It is interesting to note that in the weak flux pileup models of *Priest and Forbes* [1986], the saturation limit is less severe (the postsaturation reconnection time increases logarithmically with S [*Litvinenko et al.*, 1996; *Litvinenko*, 1999]), since the pileup scales more weakly with S; nevertheless, the pileup scaling observed in our simulations ($\approx S^{1/4}$) seems to be more consistent with the three-dimensional stagnation point flow solutions than with the two-dimensional flux pileup solutions of *Priest and Forbes* [1986]. Further, spacecraft observations demonstrate that flux pileup is rarely observed under southward IMF conditions [*Anderson et al.*, 1997; *Mozer et al.*, 2002]. It is possible that the intense current sheets observed in resistive MHD simulations eventually break up due to one or more MHD instabilities (e.g., the tearing mode or the Kelvin-Helmholtz instability) so that the current sheet becomes turbulent. Under such conditions, it might be possible to support high mean field reconnection rates in the absence of extreme levels of magnetic energy pileup. Unfortunately, limited

computational resources, which currently confine the high-resolution GGCM simulations presented in this paper to short timescales (≈2 hours) and low Lundquist numbers ($S \lesssim 5000$), prevent us from accurately modeling such small-scale turbulence.

[39] What about category 2 approaches, which seek to solve the reconnection timescale problem by appealing to kinetic theory? The most promising such approaches seem to be those which focus on the "ion scale" terms (namely, the Hall electric field and the divergence of the electron pressure tensor) in the generalized Ohm's law. We think that such an approach is likely on the right track for a number of reasons: (1) observations show that the thickness of the magnetopause current layer approaches the ion inertial scale; (2) recent reconnection modeling efforts [*Birn and Hesse*, 2001; *Kuznetsova et al.*, 2001; *Ma and Bhattacharjee*, 2001; *Otto*, 2001; *Pritchett*, 2001; *Shay et al.*, 2001] suggest that Hall electric fields permit "fast" (i.e., on Alfvénic timescales) reconnection to occur independently of the dissipation mechanism; (3) particle-in-cell simulations demonstrate that electron pressure anisotropies are likely responsible for the breaking of the frozen flux constraint in collisionless current sheets with thicknesses of the order of the ion skin depth [*Hesse et al.*, 2001a; *Hesse et al.*, 2001b; *Kuznetsova et al.*, 2001]; (4) recent analytical and numerical solutions of the resistive Hall-MHD equations [*Dorelli and Birn*, 2003; *Dorelli*, 2003] have demonstrated that when reconnection occurs in thin current sheets via the flux pileup mechanism, Hall electric fields can allow the pileup to saturate before the reconnection rate begins to stall due to the finite external plasma pressure; thus Hall electric fields allow reconnection to proceed, even in thin current sheets, at a rate which is independent of the Lundquist number (in contrast to the logarithmic dependence of the reconnection rate on S predicted by the Petschek model); (5) Hall electric fields might in some cases allow Petschek-like configurations to be realized in large systems even when the plasma resistivity is spatially uniform (as argued by *Shay et al.* [1999]); then, of course, one would not expect to observe any magnetic pileup at the subsolar magnetopause under southward IMF conditions.

[40] Points 4 and 5 are particularly compelling. Not only do they imply that the reconnection rate should be independent of the Lundquist number (making Alfvénic reconnection possible in the limit $S \rightarrow \infty$), but they both predict a reduction in the amount of magnetic pileup required to support a given magnetosheath flow (thus potentially explaining the observed lack of magnetic pileup at the terrestrial magnetopause under southward IMF conditions). For example, *Dorelli* [2003] argues that in a thin current sheet driven by a two-dimensional stagnation point flow, Hall electric fields modify the flux pileup scaling law so that the maximum upstream magnetic field, B_{up}^{max}, scales as follows:

$$B_{up}^{max} \propto E\left(\frac{S}{1 + SCd_i/\lambda C}\right)^{1/2}, \tag{24}$$

where E is the reconnection electric field, d_i is the ion inertial length, λ is the length scale associated with the stagnation point flow, and C is an arbitrary constant (which is insensitive to S and proportional to $d_i^{r+1/2}$, where $r > 0$). Thus the flux pileup saturates at a level which is insensitive to the Lundquist number. The maximum reconnection rate (corresponding to the upper limit implied by the finite external plasma pressure available to drive the reconnection) is given by:

$$E^{max} \propto \beta^{1/2}\left(\frac{1 + Sd_i/\lambda}{SC}\right)^{1/2}, \tag{25}$$

where β is the plasma beta upstream of the current sheet. Thus if $d_i \approx \lambda$ (i.e., if the scale of the stagnation flow is comparable to the ion skin depth), then Alfvénic reconnection is possible even in the limit of zero plasma resistivity (so long as β is not too small). We note that *Sonnerup and Priest* [1975] pointed out that their three-dimensional stagnation point flow solution can be extended to include the Hall and electric pressure gradient term in Ohm's law; however, in those solutions, the components of the magnetic field are assumed to be functions only of the spatial coordinate normal to the current sheet. *Dorelli* [2003] demonstrated how to include the effects of the Hall induced "bending" [*Mandt et al.*, 1994] of the magnetic field in the $\kappa = 0$ case. The authors are unaware of any Hall MHD solutions which extend this quadrupolar magnetic field solution to arbitrary κ case (i.e., to the case where the stagnation point flow is three-dimensional).

[41] Alternatively, it has been argued by *Shay et al.* [1999] that the spatial scale of the "ion inertial region", where ion bulk flows decouple from electron bulk flows, should be microscopic in both dimensions, implying that on larger scales, away from the ion inertial region, the current sheet bifurcates into a system of two current sheets (similar in structure to the Petschek slow shock configuration). The large-scale bifurcated current sheet structure observed by *Shay et al.* [1999] plays a role, similar to that played by Petschek's slow shock configuration, in decoupling the reconnection rate from the dissipation physics. A Petschek-like solution also has the desirable feature that there is no magnetic flux pileup upstream of the diffusion region (consistent with observations at the terrestrial magnetopause). Nevertheless, it is still not clear to us what physical mechanism is responsible for the large-scale bifurcation observed in the simulations of *Shay et al.* [1999]. Does whistler dispersion play an essential role in the formation of this x-type current structure, as argued by *Shay et al.* [1999]? *Biskamp et al.* [1995] has argued, for example, that the x-type current structure can be derived from the electron MHD equations (in which the ions are assumed to be a static, charge neutralizing fluid, and only the electron dynamics are followed), but the electron MHD equations apply only to very small-scale magnetic structures (where the spatial scale of the magnetic field is smaller than the ion skin depth). Recent simulations of magnetic island coalescence which treated "large" islands (where the island wavelength is much larger than the ion skin depth) [*Dorelli and Birn*, 2003] demonstrated that the whistler mediated reconnection rate can be sub-Alfvénic (being directly related to the ratio of the ion skin depth and the island wavelength, even when there are spatially localized regions with strong electron-ion decoupling). On the other hand, the recent scaling study of *Shay et al.* [2004] shows that in some cases,

reconnection appears not to be directly driven by external flows; rather, the reconnection process seems to occur in phases, with an explosive current sheet collapse phase in which the sheet bifurcates into a Petshek-like configuration. *Shay et al.* [2004] refer to this phase as the "asymptotic phase" of reconnection, arguing that the reconnection rate in the asymptotic phase is internally driven (much as Petschek reconnection is internally driven [*Forbes*, 2001]) and insensitive to external boundary conditions. Thus modern two-dimensional reconnection theory seems to have come full circle, and the issue of whether reconnection in astrophysical contexts occurs in long, thin ion inertial sheets or in microscopic Petschek-type sheets remains unresolved even in the context of two-fluid theory.

[42] Nevertheless, from a practical perspective, resistive Hall MHD and two fluid approaches (which include electron skin depth scale physics) have the virtue of being capable of simulating "mesoscale" systems which span several hundred ion skin depths, running for several hundred Alfvén times. In contrast, full particle-in-cell simulations are typically confined to simulation domains which span only several ion skin depths, running for several ion gyroperiods. Thus it is quite possible that in the next several years, as Hall MHD codes begin to make use of adaptive mesh refinement techniques, truly global Hall MHD simulations of the terrestrial magnetosphere will be possible, and, given the exciting results coming out of recent microscale simulations, such global Hall MHD simulations may finally solve the reconnection timescale problem which has been with us since the appearance of the Sweet-Parker theory almost 50 years ago.

[43] **Acknowledgments.** J.C. Dorelli acknowledges conversations with Paul Watson during a workshop at the Aspen Center for Physics in June of 2003. This work was supported by a National Research Council Postdoctoral Fellowship at the NASA Goddard Space Flight Center.

[44] Shadia Rifai Habbal thanks Eric Priest and Michael A. Shay for their assistance in evaluating this paper.

References

Anderson, B. J., T.-D. Phan, and S. A. Fuselier (1997), Relationships between plasma depletion and subsolar reconnection, *J. Geophys. Res.*, *102*, 9531–9542.

Anderson, C., and E. R. Priest (1993), Time-dependent magnetic field annihilation at a stagnation point, *J. Geophys. Res.*, *98*, 19,395–19,407.

Birn, J., and M. Hesse (2001), Geospace environment modeling (GEM) magnetic reconnection challenge: Resistive tearing, anisotropic pressure and Hall effects, *J. Geophys. Res.*, *106*, 3737–3750.

Biskamp, D. (1986), Magnetic reconnection via current sheets, *Phys. Fluids*, *29*, 1520–1531.

Biskamp, D. (1993), *Nonlinear Magnetohydrodynamics*, Cambridge Univ. Press, New York.

Biskamp, D., and E. Schwarz (2001), Localization, the key to fast magnetic reconnection, *Phys. Plasmas*, *8*, 4729–4731.

Biskamp, D., E. Schwarz, and J. F. Drake (1995), Ion-controlled collisionless magnetic reconnection, *Phys. Rev. Lett.*, *75*, 3850–3853.

Cowley, S. W. H. (1980), Plasma populations in a simple open model magnetosphere, *Space Sci. Rev.*, *26*, 217–275.

Cowley, S. W. H. (1982), The causes of convection in the Earth's magnetosphere: A review of developments during the IMS, *Rev. Geophys.*, *20*, 531–565.

Craig, I. J. D., and P. G. Watson (1999), Flare-like energy release by flux pile-up reconnection, *Solar Phys.*, *191*, 359–379.

Craig, I. J. D., R. B. Fabling, and P. G. Watson (1997), The power output of spine and fan magnetic reconnection solutions, *Astrophys. J.*, *485*, 383–388.

Crooker, N. U., T. E. Eastman, and G. S. Stiles (1979), Observations of plasma depletion in the magnetosheath at the dayside magnetopause, *J. Geophys. Res.*, *84*, 869–874.

Daughton, W. (2003), Electromagnetic properties of the lower-hybrid drift instability in a thin current sheet, *Phys. Plasmas*, *10*, 3103–3119.

Dorelli, J. (2003), Effects of Hall electric fields on the saturation of forced antiparallel magnetic field merging, *Phys. Plasmas*, *10*, 3309–3314.

Dorelli, J., and J. Birn (2003), Whistler-mediated magnetic reconnection in large systems: Flux pile-up and the formation of thin current sheets, *J. Geophys. Res.*, *108*(A3), 1294, doi:10.1029/2002JA009484.

Drake, J. F., M. Swisdak, C. Catell, M. A. Shay, B. N. Rogers, and A. Zeiler (2003), Formation of electron holes and particle energization during magnetic reconnection, *Science*, *299*, 873–877.

Dungey, J. W. (1961), Interplanetary magnetic field and the auroral zones, *Phys. Rev. Lett.*, *6*, 47–48.

Evans, C. R., and J. F. Hawley (1988), Simulation of magnetohydrodynamic flows: A constrained transport method, *Astrophy. J.*, *332*, 659–677.

Fabling, R. B., and I. J. D. Craig (1996), Exact solutions for steady-state, planar, magnetic reconnection in an incompressible viscous plasma, *Phys. Plasmas*, *3*, 2243–2247.

Fitzpatrick, R. (2003), Scaling of forced magnetic reconnection in the Hall-magnetohydrodynamic Taylor problem, *Phys. Plasmas*, *11*, 937–946.

Forbes, T. G. (2001), The nature of Petschek-type reconnection, *Earth Planets Space*, *53*, 424–429.

Gosling, J. T., M. F. Thomsen, S. J. Bame, R. C. Elphic, and C. T. Russell (1990), Plasma flow reversals at the dayside magnetopause and the origin of asymmetric polar cap convection, *J. Geophys. Res.*, *95*, 8073–8084.

Harten, A., and G. Zwas (1972), Self-adjusting hybrid schemes for shock computations, *J. Comput. Phys.*, *9*, 568–583.

Hesse, M., K. Schindler, J. Birn, and M. Kuznetsova (1999), The diffusion region in collisionless magnetic reconnection, *Phys. Plasmas*, *6*, 1781–1795.

Hesse, M., J. Birn, and M. Kuznetsova (2001a), Collisionless magnetic reconnection: Electron processes and transport modeling, *J. Geophys. Res.*, *106*, 3721–3735.

Hesse, M., M. Kuznetsova, and J. Birn (2001b), Particle-in-cell simulations of three-dimensional collisionless magnetic reconnection, *J. Geophys. Res.*, *106*, 29,831–29,841.

Heyn, M. F., and V. S. Semenov (1996), Rapid reconnection in compressible plasmas, *Phys. Plasmas*, *3*, 2725–2741.

Heyn, M. F., H. K. Biernat, R. P. Rijnbeek, and V. S. Semenov (1988), The structure of reconnection layers, *J. Plasma Phys.*, *40*, 235–252.

Horiuchi, R., W. Pei, and T. Sato (2001), Collisionless driven reconnection in an open system, *Earth Planets Space*, *53*, 439–445.

Kennel, C. F. (1995), *Convection and Substorms: Paradigms of Magnetospheric Phenomenology*, Oxford Univ. Press, New York.

Kuznetsova, M. M., M. Hesse, and D. Winske (2001), Collisionless reconnection supported by nongyrotropic pressure effects in hybrid and particle simulations, *J. Geophys. Res.*, *106*, 3799–3810.

Lapenta, G., J. U. Brackbill, and W. S. Daughton (2003), The unexpected role of the lower hybrid drift instability in magnetic reconnection in three dimensions, *Phys. Plasmas*, *10*, 1577–1587.

Li, H., K. Nishimura, D. C. Barnes, S. P. Gary, and S. A. Colgate (2003), Magnetic dissipation in a force-free plasma with a sheet-pinch configuration, *Phys. Plasmas*, *10*, 2763–2771.

Lin, Y. (2001), Global hybrid simulation of the dayside reconnection layer and associated field-aligned currents, *J. Geophys. Res.*, *106*, 25,451–25,465.

Litvinenko, Y. E. (1999), The pressure limitations on flux pile-up reconnection, *Solar Phys.*, *186*, 291–300.

Litvinenko, Y. E., T. G. Forbes, and E. R. Priest (1996), A strong limitation on the rapidity of flux pile-up reconnection, *Solar Phys.*, *167*, 445–448.

Ma, Z. W., and A. Bhattacharjee (1996), Fast impulsive reconnection and current sheet intensification due to electron pressure gradients in semi-collisional plasmas, *Geophys. Res. Lett.*, *23*, 1673–1676.

Ma, Z. W., and A. Bhattacharjee (2001), Hall magnetohydrodynamic reconnection: The geospace environment modeling challenge, *J. Geophys. Res.*, *106*, 3773–3782.

Mandt, M. E., R. E. Denton, and J. F. Drake (1994), Transition to whistler mediated magnetic reconnection, *Geophys. Res. Lett.*, *21*, 73–76.

Mozer, F. S., S. D. Bale, and T. D. Phan (2002), Evidence of diffusion regions at a subsolar magnetopause crossing, *Phys. Rev. Lett.*, *89*, 015,002.

Mozer, F. S., T. D. Phan, and S. D. Bale (2003), The complex structure of the reconnecting magnetopause, *Phys. Plasmas*, *10*, 2480–2485.

Oieroset, M., T. Phan, M. Fujimoto, R. Lin, and R. Lepping (2001), In situ detection of collisionless reconnection in the earth's magnetotail, *Nature*, *412*, 414–417.

Omidi, N., and D. Winske (1995), Structure of the magnetopause inferred from one-dimensional hybrid simulations, *J. Geophys. Res.*, *100*, 11,935–11,955.

Onsager, T. G., and M. Lockwood (1997), High-latitude particle precipitation and its relationship to magnetospheric source regions, *Space Sci. Rev.*, *80*, 77–107.

Otto, A. (2001), Geospace environment modeling (GEM) magnetic reconnection challenge: MHD and Hall MHD: Constant and current dependent resistivity models, *J. Geophys. Res.*, *106*, 3751–3757.

Parker, E. N. (1957), Sweet's mechanism for merging magnetic fields in conducting fluids, *J. Geophys. Res.*, *62*, 509.

Parker, E. N. (1973), Comments on the reconnexion rate of magnetic fields, *J. Plasma Physics*, *9*, 49–63.

Paschmann, G. (1997), Observational evidence for transfer of plasma across the magnetopause, *Space Sci. Rev.*, *80*, 217–234.

Paschmann, G., et al. (1979), Plasma acceleration at the earth's magnetopause: Evidence for reconnection, *Nature*, *282*, 243–282.

Petschek, H. E. (1964), Magnetic field annihilation, in *AAS-NASA Symposium on Physics of Solar Flares*, *NASA Spec. Publ. 50*, pp. 425–439, NASA, Washington, D.C.

Priest, E. R. (1996), Reconnection of magnetic lines of force, in *Solar and Astrophysical MHD Flows*, edited by K. Tsinganos, pp. 151–170, Kluwer Acad., Norwell, Mass.

Priest, E. R., and T. G. Forbes (1986), New models for fast steady state magnetic reconnection, *J. Geophys. Res.*, *91*, 5579–5588.

Priest, E. R., and T. G. Forbes (2000), *Magnetic Reconnection: MHD Theory and Applications*, pp. 123–125, chap. 4, Cambridge Univ. Press, New York.

Pritchett, P. L. (2001), Geospace environment modeling magnetic reconnection challenge: Simulations with a full particle electromagnetic code, *J. Geophys. Res.*, *106*, 3783–3798.

Raeder, J. (1999), Modeling the magnetosphere for northward interplanetary magnetic field: Effects of electrical resistivity, *J. Geophys. Res.*, *104*, 17,357–17,367.

Raeder, J., et al. (2001), Global simulation of the geospace environment modeling substorm challenge event, *J. Geophys. Res.*, *106*, 381.

Scudder, J. D., F. S. Mozer, N. C. Maynard, and C. T. Russell (2002), Fingerprints of collisionless reconnection at the separator: 1. Ambipolar-Hall signatures, *J. Geophys. Res.*, *107*(A10), 1294, doi:10.1029/2001JA000126.

Semenov, V. S., O. A. Drobysh, and M. F. Heyn (1998), Analysis of time-dependent reconnection in compressible plasmas, *J. Geophys. Res*, *103*, 11,863–11,873.

Shay, M. A., and J. F. Drake (1998), The role of electron dissipation on the rate of collisionless magnetic reconnection, *Geophys. Res. Lett.*, *25*, 3759–3762.

Shay, M. A., J. F. Drake, and B. N. Rogers (1999), The scaling of collisionless, magnetic reconnection for large systems, *Geophys. Res. Lett.*, *26*, 2163–2166.

Shay, M. A., J. F. Drake, B. N. Rogers, and R. E. Denton (2001), Alfvénic collisionless magnetic reconnection and the Hall term, *J. Geophys. Res.*, *106*, 3759–3772.

Shay, M. A., J. F. Drake, M. Swisdak, and W. Dorland (2003), Inherently three dimensional magnetic reconnection: A mechanism for bursty bulk flows?, *Geophys. Res. Lett.*, *30*(6), 1345, doi:10.1029/2002GL016267.

Shay, M. A., J. F. Drake, M. Swisdak, and B. N. Rogers (2004), The scaling of embedded collisionless reconnection, *Phys. Plasmas*, *11*, 2199–2213.

Song, P., and C. T. Russell (2002), Flow in the magnetosheath: The legacy of John Spreiter, *Planet. Space Sci.*, *50*, 447–460.

Song, P., C. T. Russell, and M. F. Thomsen (1992), Slow mode transition in the frontside magnetosheath, *J. Geophys. Res.*, *97*, 8295–8305.

Sonnerup, B. U. O. (1995), Fluid aspects of reconnection at the magnetopause: In situ observations, in *Physics of the Magnetopause*, *Geophys. Monogr. Ser.*, vol. 90, edited by P. Song, B. U. O. Sonnerup, and M. F. Thomsen, pp. 167–180, AGU, Washington, D. C.

Sonnerup, B. U. O., and E. R. Priest (1975), Resistive MHD stagnation-point flows at a current sheet, *J. Plasma Phys.*, *14*, 283–294.

Strachan, N. R., and E. R. Priest (1994), A general family of non-uniform reconnection models with separatrix jets, *Geophys. Astrophys. Fluid Dyn.*, *74*, 245–274.

Sweet, P. A. (1958), The neutral point theory of solar flares, in *Electromagnetic Phenomena in Cosmic Physics*, edited by B. Lehnert, pp. 123–134, Cambridge Univ. Press, London, New York.

Wang, X., Z. W. Ma, and A. Bhattacharjee (1996), Fast magnetic reconnection and sudden enhancement of current sheets due to inward boundary flows, *Phys. Plasmas*, *3*, 2129–2134.

Wang, X., A. Bhattacharjee, and Z. W. Ma (2001), Scaling of collisionless forced reconnection, *Phys. Rev. Lett.*, *87*, 1–4.

Wang, Y. L., J. Raeder, and C. T. Russell (2003), Plasma depletion layer: Event studies with a global code, *J. Geophys. Res.*, *108*(A1), 1010, doi:10.1029/2002JA009281.

Watson, P. G., and I. J. D. Craig (1997), Analytic solutions of the magnetic annihilation and reconnection problems. ii Three-dimensional flows, *Phys. Plasmas*, *4*, 110–119.

Wu, C. C. (1992), MHD flow past an obstacle: Large-scale flow in the magnetosheath, *Geophys. Res. Lett.*, *19*, 87–90.

J. C. Dorelli, M. Hesse, M. M. Kuznetsova, and L. Rastaetter, Electrodynamics Branch, Laboratory for Extraterrestrial Physics, NASA Goddard Space Flight Center, Greenbelt, MD 20771, USA. (john.dorelli@unh.edu; michael.hesse@gsfc.nasa.gov)

J. Raeder, Space Science Center, University of New Hampshire, 39 College Road, Durham, NH 03824, USA. (jraeder.igpp.ucla.edu)